



## **1. Introduction**

The investigation included metallography, hardness testing and fractography. The results have shown that the material was in a good condition and the main cause of this fracture was FOD induced notch which acted as a stress raiser. SEM/EDX analysis was also applied on the notched area. The source of foreign object was found to be silicon base earth elements. Both fractographic and metallographic tests displayed no corrosion evidence (IGA, uniform corrosion etc.), neither on the fractured area nor on the rest of the outer surface of the part. Also the paint was intact with undercoat on the notched area. Therefore it was established that, the fatigue crack has propagated only with mechanical manner. Complete notch shape could not be retrieved due to missing part on the blade. To avoid recurrence of the failure, visual and non destructive inspections may be performed more tediously with shorter interval times.

## **2. Propeller background**

The Model 185 Skywagon is basically a 180 with a more powerful engine and was first flown in 1960. In 1962, the US Air Force selected the Model 185 to supply countries eligible for Military assistance. This variant

was designated the U-17 [1]. As shown in Fig. 1, it has a single engine and propeller attached at the front of the airframe. The propeller assembly, consisting of two blades and a hub, was attached to the engine crankshaft [2].

As shown in Fig. 2, One of the propeller blades of presently used mono-propeller U-17B airplanes was broken off during the flight. Propeller was a high strength 2024 aluminium alloy which is a commonly used material in aviation due to its advantages of resistant to crack growth, good repairability, perfect damage tolerance properties [4].

Assembling of the propeller was carried out in 1970. Total service life was 35 years with a 1850 hours flight. During the service life, various controls were utilized in certain periods. The control operations applied on the propeller include the disassembling from airplane, after removing its paint, evaluation of the physical failures like scratch and the collapses which are resulted from the strikes of sand and stones and the investigation of the crack propagation (formation) on the surface by fluorescent penetration method. Maintenance reports revealed that the propeller was last no-destructive tested in 2001, at 50 flight hours prior to the accident.

### 3. The situation of failure propeller

It was determined that one third of the total length of the blade was left on the lane whereas the rest was removed after breaking off. As shown in Fig. 3, on the surface of the blade it was determined that several deformed areas were formed as a result of impact effect. As shown in Fig. 4, crack surface investigations on the deformed surface did not show any intensive corrosion, dirt, lubricant layer, colour change or oxidation. Residual shape deformations (e.g. shrinkage, bending, etc.) were not determined on the remaining part of the blade.



Fig. 1. General appearance of Cessna 185 [3].



Fig. 2. General appearance of broken propeller blade.



Fig. 3. Surface of the failure blade.



Fig. 4. Crack surface.

#### 4. Definition of failure mechanism

For the fundamental understanding of the crack mechanism on the blade, both the general condition of the removed piece and the crack surface is required to be investigated. For this purpose, crack surface was investigated in detail by stereo and scanning electron microscopes (SEM). General evaluation was confirmed by these microscopic investigations showing that corrosion was not occurred on the crack surface. Crack was occurred on two different surfaces in an area including the propeller leading edge during the axis normal to the propeller (zone I) and on the rest part including the propeller trailing edge during the axis having  $45^\circ$  angle with the propeller (zone II). It was observed that zone I contains straight smooth planes and has less roughness resulting in better light reflection ability whereas zone II has more roughness and has less light reflection. Hence zone I has a bright and zone II has a matte appearance (Fig. 5). When the surface areas of zone I and zone II are rated, the half portion of the fracture surface has been formed with fatigue.

Zone I crack surface investigations showed that cyclic loads caused fatigue striations and stop lines. As can be shown in Fig. 6, the fatigue striations have characteristic semi elliptic circles that formed and propagated under cyclic loads. In this examination it was revealed that the fracture surfaces did not display evidence of corrosion products.

Center of the ellipse and the starting point of the crack is reached by following the gradually shrinking rings. After the determination of the crack zone by this method, starting point was examined by SEM. It was determined that, crack was started on the back outer surface of the blade and located in an area having



Fig. 5. Zone I and zone II on crack surface.



Fig. 6. Zone I "semi elliptic" fatigue striations (Mag. 250 $\times$ ).

a dent type deformed surface. Moreover, the residues, such as paint, were not observed on the areas close to the outer surface and dent dimension was measured with a depth of 140  $\mu\text{m}$  and a width of 3060  $\mu\text{m}$ . It was also observed that fatigue striations just start at this zone. Outer surface of the deformed zone which includes

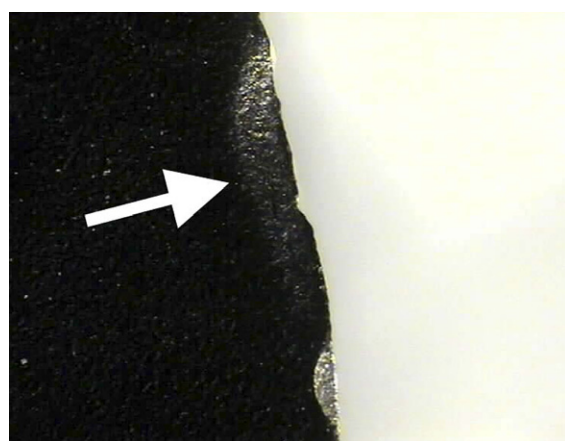


Fig. 7. Appearance of "dent damage" under stereo microscope (Mag. 16 $\times$ ).



Fig. 8. Appearance of backscattered SEM image of crack initiation site (Mag. 65 $\times$ ).

crack starting point revealed that the surface is covered by the paint. These observations can be seen stereoscopic and backscattered SEM images in Figs. 7 and 8, respectively.

Fatigue damage generally starts at the surface and the faulty areas having sharp edges, scratches, notch or burr where the local stresses are high. In the view of blade fatigue investigation, it is discovered that, fatigue started at the back surface where the tension and bending type stresses take place especially at the dent area which act as a stress raiser. Surface dents increase the stress locally by the geometric and metallurgical aspects. Geometrically, it causes notch effect by the formation of microcracks and/or formation of interrupted surface. And since it was formed by an impact, metallurgically, the impact effect on this zone has resulted in the increase of hardness and the decrease of ductility.

As it mentioned before, the blade has been known to be inspected in regards of dent/nick type defects in 2001, 50 h before the failure. Additionally, the paint on the blade has been removed and NDI inspection has been performed. As the crack initiation zone is open to surface and the fracture surfaces display no paint traces, it is highly possible that the crack did not exist at the time of last scheduled NDI or the crack was a microcrack in which the paint could not penetrate with capillary effect. These microcracks can be very small that can not be seen even by using NDI inspection [5]. The dent on the surface was painted which told us it is likely that had been exist at the time of inspection. Two different approaches have been used to figure out whether the possibility of dent formation due to impact effect, could be formed without removing the paint. In the first approach, a dent zone has been formed manually with the more possible stone that has been thought to hit the blade. As a result the paint has been removed with the impact damage. In the second approach, the flexibility capacity of the paint has been tested by manually deforming the surface using the hardness test apparatus using brinell hardness indenter. The paint did not display any evidence of spalling,

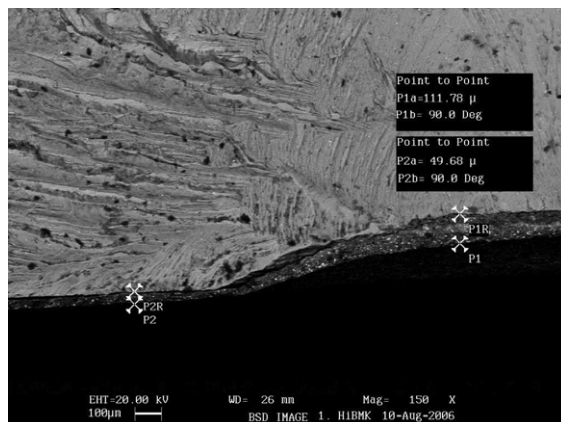


Fig. 9. Paint plus undercoat thicknesses in backscattered SEM image of crack initiation site (Mag. 150 $\times$ ).

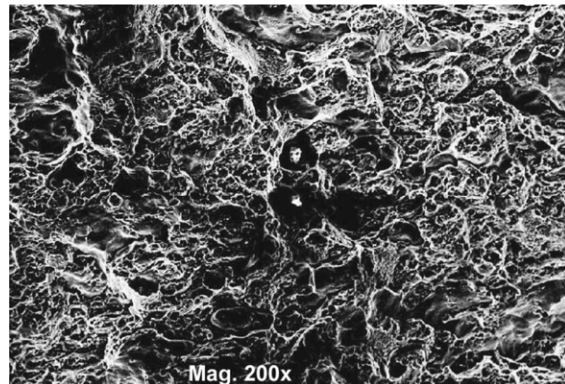


Fig. 10. SEM image of zone II which contains equi axial dimples (Mag. 200 $\times$ ).

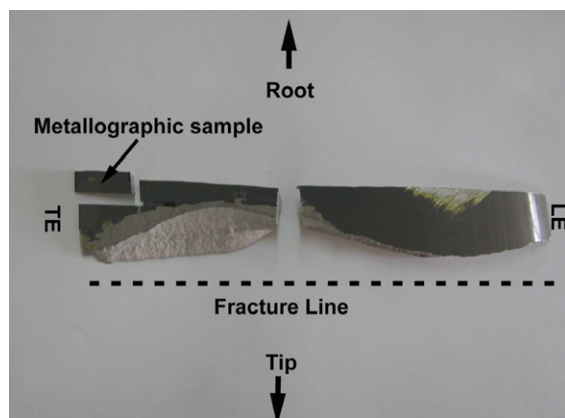


Fig. 11. Metallographic sample location.

deformation on the paint at the result. Paint thickness in dent area was measured by SEM images. As can be seen in Fig. 9, the nominal paint plus undercoat thickness in outer surface was 50  $\mu\text{m}$ , whereas the paint thickness in dent area was 112  $\mu\text{m}$ .

The inspection of fracture surfaces of zone II, revealed on overload failure due to monotonic loads.

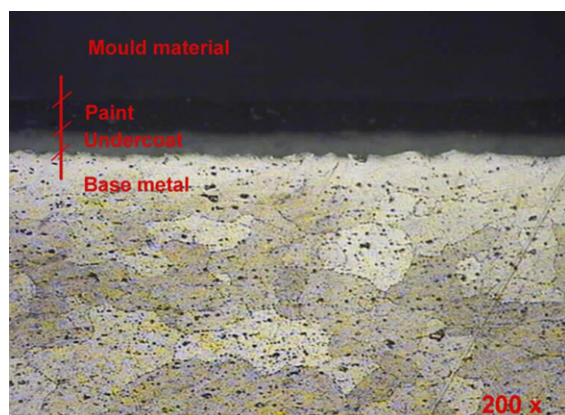


Fig. 12. Metallographic sample under optical microscope (Mag. 200 $\times$ ).

The detailed inspection fracture surface of zone II has revealed that the fracture was a ductile type fracture, mostly due to tensile stress containing equi axial dimples in [Fig. 10](#).

Metallographic evaluation was also used to obtain more detailed information about blade. The transverse section cut from the trailing edge near the fracture surface. In [Fig. 11](#), The location of section to be prepared can be seen.

Microstructural evaluations performed with reflected light optical microscope. As a result of this evaluation, the general condition of undercoat and paint was found to be good with no evidence of cracks, spalling. Also, the blade material has in good condition that neither IGA nor any other corrosion type found. The paint and undercoat thicknesses was measured from this metallographic section and average undercoat thickness 20  $\mu\text{m}$ , average paint thickness 28  $\mu\text{m}$  values which well-matched with SEM observations were obtained. In [Fig. 12](#) the general appearance of microstructure was given.



493905

Propeller blade used in mono-propeller U-17B airplanes was broken during a flight. The material that was used was aluminum alloy 2024 which is commonly used in airplanes. The service life for this propeller was 35 years with 1850 hours of flight. After the failure, the airplane was disassembled, and different parts of the blade were analyzed using various methods.

The means of investigation that were used in the analysis were hardness testing, metallography, fractography using SEM, and light optical microscope for evaluating microstructure. Non-destructive inspecting was also used. Computational methods were not used.

Using SEM, the analysis obtained fractographic figures from the crack propagation surface. Using a light optical microscope, the analysis obtained figure showing the dent damage that was assumed as the reason for the crack initiation. Furthermore, metallographic evaluation of the blade sample was obtained which showed the fracture line along the blade. While the article mentions using hardness tests, no actual results from these tests are provided in the analysis.

The primary cause for the failure according to the analysis was that the blade crack had initiated through FOD (Foreign Object Damage). And then through fatigue caused by cyclic load from wind propagated the crack and the failure happened. Looking at the fractographic figures provided in the analysis, we can see that there is ductile type of fracture surface in the form of dimples. This would indicate some ductile nature for the fracture. Also looking at the microscopic figures, we can see dents in the surface of the crack initiation site which would support the analysis theory that there was a dent caused by some external object or mechanism. The most evident evidence of fatigue failure is provided in figure 6. Where some semi-elliptical fatigue striations can be seen in the fracture surface. In addition, according to the non-destructive inspecting that was done multiple times during the service life of the plane, the plane did not have any cracks on the surface. Therefore, the likelihood that the crack initiation was caused by external object causing damage to the blade during the flight is high. Although, the analysis does mention that non-destructive inspection might not see microcracks in the paint, which could also cause the failure. In the event of this the analysis does two approaches to exclude the possibility. First is manually forming a dent zone due to impact effect and second is using hardness tests to manually deform the surface. According to the results, the paint did not display behavior that would indicate that it would be faulty. Lastly, the microstructure of the paint was investigated using light optical microscope and there was no indication of the paint being in poor condition. Corrosion was disregarded due to fractographic figures not showing traits that are common with corrosion such as oxidation of grain boundaries. The hypothesis that was provided in the analysis seems to be likely.

Plastic deformation cannot be ruled out. The localized stress caused in the dent of the blade can cause plastic deformation in the blade.

Creep can be ruled out. It is not likely that the airplane would be subjected to temperatures high enough to cause creep damage in the material.

Based on the figures provided in the analysis, brittle fracture can be ruled out. There seems to be no indication of brittle fracture characteristics in the fractographies. However, with more fractographic investigation there could be a possibility for small amounts of brittle fracture characteristics to be found.

Fatigue seems to be the most likely failure mechanism that happened. Aluminum is susceptible to fatigue damage and a dent in the blade would probably suffice as a crack initiation point. The wind causes a load high enough to be able to propagate a crack.

The other option for the failure seems to be environmentally assisted failure. While corrosion was ruled out by the analysis, there is not enough evidence to completely rule it out. The dimples in figure 10 could be caused by corrosion. And the mechanism for the failure could have both corrosion and fatigue. The fractographies also seem to have black spots which are hard to analyze but they could be corrosive pits. Stress corrosion cracking is highly likely since the airplane is subjected to high amounts of oxygen and other corrosive substances that the atmosphere has. A second scenario for the failure could have been that the blade was damaged by the dent caused from external object. The paint would then be damaged, and corrosive substance would start to form in the dent. Combination of corrosive atmosphere with the localized stress in the dent would then cause a crack to initiate and then propagate. Stress corrosion cracking is probably as likely as the fatigue failure in this scenario. However, it is less likely that the blade was already corroded before the dent based on the results that the paint of the blade was in good condition.

It is hard to prevent such an occurrence in an airplane. External damage is random and can be caused through sheer bad luck. The material could be protected better through higher concentration of steel, but it would lower the performance of the blade overall. Non-destructive tests could be made after each flight, but it would be expensive, and the crack would still be able to initiate and propagate during the same flight. Better material is always an option, but it is more expensive and not a guarantee that the failure would not happen again. Flying in safe conditions is preferable but even in safe conditions random accidents can occur. Perhaps with the combination of all of the above the chances for the accident to happen would be extremely low, but still theoretically possible.

549707

## 1 Background

The article investigates a fracture of a propeller blade in Cessna 185 Skywagon. The propeller had 1850 total service hours, and it had been inspected by liquid penetrant inspection 50 flight hours prior to the failure. No cracks were found in the inspection.

## 2 Investigation methods

Fracture surface and a metallographic sample prepared from the propeller blade near the fracture surface were investigated using optical and electron microscopy, and visual inspection. Visual examination of the fracture surface revealed two distinct areas: Zone I, which was relatively flat but matte in appearance, and Zone II, which was more reflective and had clear beachmarks.

Electron microscopy confirmed that Zone I had equiaxial dimples, suggesting ductile tearing. The beachmarks originated from a dent on the propellers surface, which was found to contain silicon using EDS, suggesting that the dent had been created by a sand particle hitting the propeller. Paint and undercoating were confirmed to be intact, which suggests that the dent was present when the propeller was inspected and repainted 50 hours before the failure. No signs of corrosion were found.

## 3 Primary cause

The failure was caused by a fatigue crack that was initiated by a surface notch caused by a grain of sand or another similar particle impacting the propeller. The propeller of the airplane rotates at over 2000 RPM during flight, which leads to millions of load cycles during the 50 flight hours that had passed after latest inspection. This is sufficient time for a fatigue crack to develop. Final fracture (Zone I) is ductile tearing caused by overloading after the cross-sectional area of the propeller had decreased enough.

## 4 Alternative mechanisms

No evidence of the blade being bent or otherwise plastically deformed, but the authors of the article did not have the full blade available for investigation, as the part the broke off was lost. Therefore, plastic deformation cannot be completely ruled out.

Creep would require elevated temperatures or very high loading to occur for extended periods, and these factors should not be present in the operating environment of an airplane propeller, which allows ruling out creep.

Paint and undercoat were intact around the entire fracture surface, so environmentally assisted failure is not very likely.

## 5 Preventing further similar failures

The inspection interval is too high considering that the propeller is subjected to cyclic loading at high frequency. It experiences millions of load cycles between inspections, which is enough for fatigue cracks to develop from initiation to final fracture between inspections, which is not acceptable for such a critical component. The inspection interval should be lowered, and additional visual inspections to identify damage that could act as an initiation site for a fatigue crack should be implemented.



## 1. Introduction

The crankshaft is a structural component which converts the linear piston movement into rotary motion while the force connecting rod is transformed to torque. Several researchers have been studied on the failed shafts [1–4]. Recently, researchers indicate that mechanical fatigue produced by cyclic bending load on the fillets and steady torsion were probably the most common cause of crankshafts failure [5–10]. Zhang and Yin [11] have investigated a wind turbine main shaft and the results show that stress concentration on the shaft surface are the main reasons that result in fracture of the main shaft. Bugarin [12] has studied two shafts and found that a larger-size fillet can minimize stress concentration in the dangerous sections which shows that the fatigue life can be significantly increased with a simple change in the structural details. Because the fracture failure of the crankshaft can affect the normal work of the machine, the failure analysis of crankshaft have a very important theoretical and practical significance. This paper finds out the cause of the crankshaft fracture through the failure analysis of the crankshaft (Fig. 1), so as to guide the design and production, improve the fatigue strength and the work reliability of the crankshaft.

In this paper, the crankshaft is made of 42CrMo steel with forging, heat treatment and nitridation. The crankshaft occurred fracture failure after using a period of time. The fracture position and surface of the crankshaft is shown in Figs. 2 and 3. The region around the lubrication hole is rough by observing Fig. 3.

## 2. Investigation into the cause of main shaft fracture

In order to analyze the cause of crankshaft fracture thoroughly, three parts of study were carried out: (1) experimental analysis of the crankshaft, (2) analysis of macroscopic feature and microstructure of the crankshaft, and (3) theoretical calculations.



(a) the air compressor



(b) the crankshaft

**Fig. 1.** Picture of the air compressor.

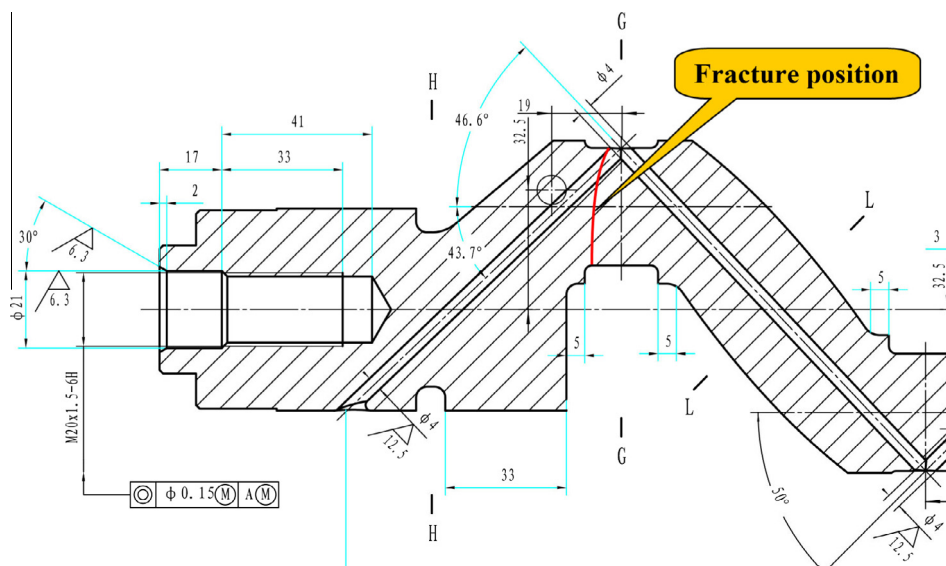


**Fig. 2.** The fracture position of the crankshaft.

## 2.1. Experimental analysis of the crankshaft

### 2.1.1. Chemical composition detection

The chemical element analysis is to accurately determine the elements content of the crankshaft material and compared it with the standard values, then determines whether the crankshaft material is suitable.

Chemical analysis of the fractured crankshaft material was carried out using a spectrometer. Examination of chemical composition of the samples taken at the point of fracture was carried out. [Table 1](#) gives the chemical composition of the crankshaft and the standard composition of 42CrMo.

As shown in [Table 1](#), obviously, the chemical composition of the main shaft is in accordance with the requirements of 42CrMo steel.

### 2.1.2. Mechanical properties test

The test results of mechanical properties including  $\sigma_b$  (Tensile strength),  $\delta$  (Reduction of area) and hardness shown in [Table 2](#).



**Fig. 3.** The fracture surface of the crankshaft.

**Table 1**  
Chemical compositions (%).

Element	Specification	Actual
C	0.38–0.45	0.41
Cr	0.90–1.20	0.95
Mo	0.15–0.25	0.15

**Table 2**  
Mechanical properties.

Test items	$\sigma_b$ (N/mm <sup>2</sup> )	$\delta$ (%)	Hardness(HRC)
Standard value	≥900	≥12	27–32
Measured value	915	14.5	31

## 2.2. Macroscopic analysis

The fracture surface shown in Fig. 4 can be divided into three regions: (1) fatigue crack initiation region, (2) fatigue expansion region and (3) static fracture region.

The catastrophic fracture which shows the fatigue crack growth rate is high seems to be a consequence of a high bending according to the Fig. 4. The reasons why the bending loading is too high is that the misalignment of main journals and the small fillet of the lubrication hole. Under the above two cases which can generate high bending stress concentration, the fatigue crack initiated on the edge of the lubrication hole and finally fractured.

The presence of beach marks with semi-elliptical shape surrounding fatigue crack initiation region indicates its expansion. These beach marks, also named progression marks were extremely important to describe fatigue fractured surfaces,

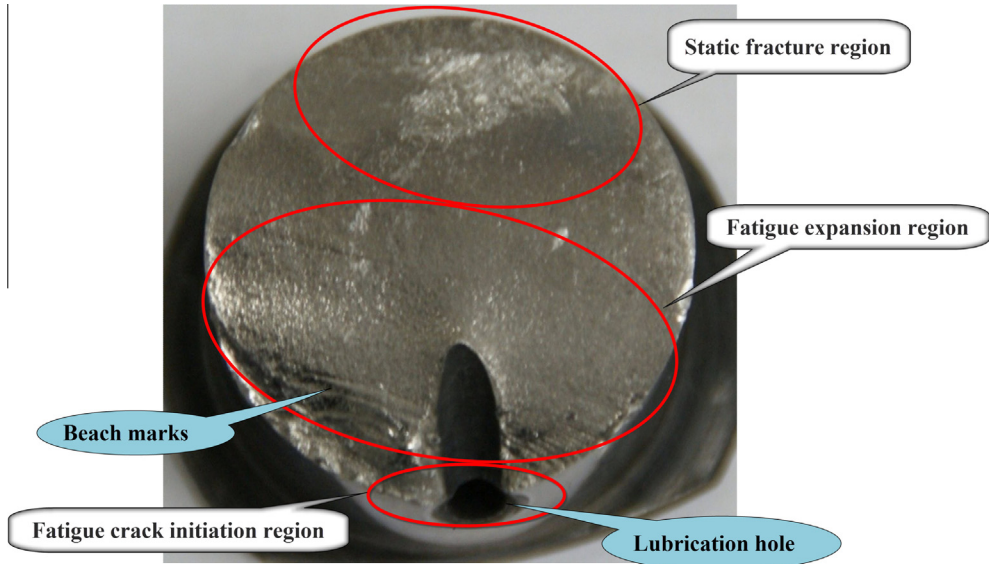


**Fig. 4.** Macro-photograph of the fracture surface.

but the beach marks are only the characteristics of the fatigue fracture and some fatigue fracture did not have obvious beach marks. The beach marks are a consequence of small overloads as a result of starting or stopping of compressor. The beach marks are really important to determine the fatigue crack growth rate and also to determine where the focus of the semi-ellipses (the crack initiation site) exists.

In the fatigue expansion region, the beach marks observed in the beginning of the expansion region resulted of the starting or stopping of the compressor operation.

The static fracture region is the portion of the structure where the final catastrophic failure occurs.

According to the above analysis, the crankshaft fracture process is as follows:

In a certain rotating cycle after a period time of normal work, micro cracks due to high bending stress concentration appeared on the fillet of lubrication hole, but the crankshaft can still close to normal working condition. As the lengthening of working time, the crankshaft began to appear obvious fluctuation with the fatigue crack extending gradually to static fracture region and then fractured completely. At the moment of fracture, friction collision happened between the two fracture surfaces, which lead to a certain degree of damage on the surfaces.

From the macroscopic analysis: The fatigue zone was formed by gradual extension of the crack source.

### 2.3. Microscopic analysis

The microscopic observation of the fracture surface was carried out using Scanning Electron Microscopy (SEM) due to its high resolution and high magnifications. By the microscopic observation and analysis, we can accurately confirm the fracture type and the initiation of crack source region, its propagation and the cause of possible fracture.

The observation points numbered 1–9 are shown in Fig. 5. However, only display of those critical observation points are shown in Fig. 6, numbered 1, 2, 4, 5, 6 and 9.

Point 1 is located on the edge of the fracture surface which is shown in Fig. 6(a). The display of the rough surface which means the point 1 is located in the static fracture region.

Point 2 is located at the static fracture region. The picture shows clearly the typical morphology of fast fracture.

Point 4 is located on the surface of the lubrication hole. The relatively smooth surface shown in Fig. 6(c) means there is no stress concentration.

Point 5 is on beside of the lubrication hole. The obvious beach marks distributed in Fig. 6(d) meaning that this is a typical fatigue expansion region.

Point 6 is located on the edge of the lubrication hole. There are three pictures in different magnification to understand the morphology of the point 6 clearly. Fig. 6(e) shows a smooth surface and we can make sure the point 6 is on the fatigue source region. We can also find out the fatigue crack initiation site by tracing back the beach marks.

Point 9 is located at the fatigue expansion region and the morphology of point 9 seems to show an occasional beach mark.

According to the above analysis, a preliminary conclusion can be drawn that the crack on the edge of the lubrication hole is the cause of the fracture of the crankshaft.

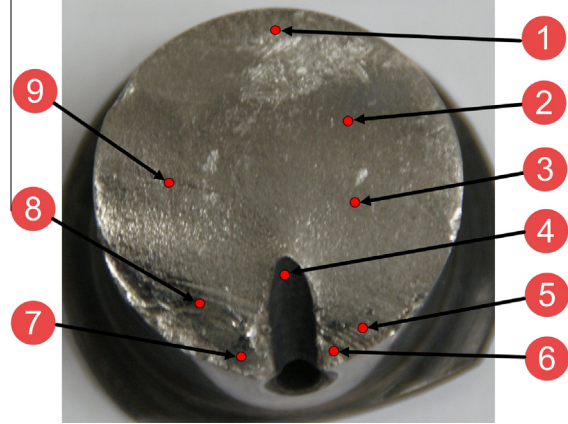


**Fig. 5.** Observation points of the fracture surface under SEM.

#### 2.4. Theoretical calculation

According to the force condition of the crankshaft when it is working, the dangerous sections are the surface of the lubrication hole and the transition fillet of journal.

##### 2.4.1. Fatigue strength checking on lubrication hole

Mechanical part theoretically able to bear force must be greater than its actual force, and the ratio of the limit stress and the allowable stress is called safety factor. In the fatigue strength design, we use fatigue limit replace the limit stress and the safety factor is determined according to design experience.

The calculation of the safety factor on the lubrication hole is obtained, as follows [13]:

$$S_{ca} = \frac{\sigma_{-1}\varepsilon_\sigma}{K_\sigma\eta\sigma_a + K_\tau\eta_\tau\tau_a + \psi_\sigma(\eta\sigma_m + \eta_\tau\tau_m)} \quad (1.1)$$

In order to calculate the safety factor, the meanings of the parameters in above calculation must be known and the calculations to obtain the parameters is as follows:

$$\begin{cases} K_\sigma = \frac{K_{t\sigma}}{0.88+AQ^b} \\ K_\tau = \frac{K_{t\tau}}{0.88+AQ^b} \\ Q = \frac{4.6}{d} \end{cases} \quad (1.2)$$

Here,  $K_\sigma$  and  $K_\tau$  are the effect coefficients of lubrication hole under bending and torsion,  $K_{t\sigma}$  and  $K_{t\tau}$  are the theoretical stress concentration factors under bending and torsion,  $Q$  is relative stress gradient,  $d$  is diameter of crankshaft pin,  $A$  and  $b$  are constants related to the heat treatment where  $A = 0.290$ ,  $b = 0.152$ ,  $\eta$  and  $\eta_\tau$  are relative stress strength factors,  $\varepsilon_\sigma$  and  $\varepsilon_\tau$  are size factors,  $\psi_\sigma$  and  $\psi_\tau$  are stress convert factors,  $\sigma_a$  and  $\sigma_m$  are working stress of the crankshaft under bending,  $\tau_a$  and  $\tau_m$  are working stress of the crankshaft under torsion,  $S_{ca}$  is safety factor.

We can get the following parameters,  $K_{t\sigma}$ ,  $K_{t\tau}$ ,  $\eta$  and  $\eta_\tau$  according to the Standard Hand book of Machine Design, and then obtain the curve of theoretical stress concentration factor and the curve of the relative stress strength factor on lubrication hole through MATLAB simulation which is shown in Figs. 7 and 8.

According to the known parameters of the crankshaft, the relationship between the safety factor and the diameter of lubrication hole after fillet has been obtained, which is shown in Fig. 9. The parameter  $a$  represents diameter of the lubrication hole after fillet in Fig. 9.

According to the part drawing where  $a = \varphi 5$  mm,  $d = \varphi 32$  mm, the safety factor  $S_{ca} = 2.477$  has been got from Fig. 9, and then we know that the fatigue strength on the lubrication hole is in allowable range which is  $[S_{ca}] = 2.0\text{--}3.0$ .

##### 2.4.2. Fatigue strength checking on the transition fillet of the journal

The calculation of the safety factor on transition fillet of the journal is as follows:

$$\begin{cases} S_\sigma = \frac{\sigma_{-1}\varepsilon_\sigma}{K_\sigma\beta\sigma_a + \psi_\sigma\beta\sigma_m} \\ S_\tau = \frac{\tau_{-1}\varepsilon_\tau}{K_\tau\beta\tau_a + \psi_\tau\beta\tau_m} \\ S_{ca} = \frac{S_\sigma S_\tau}{\sqrt{S_\sigma^2 + S_\tau^2}} \end{cases} \quad (2.1)$$

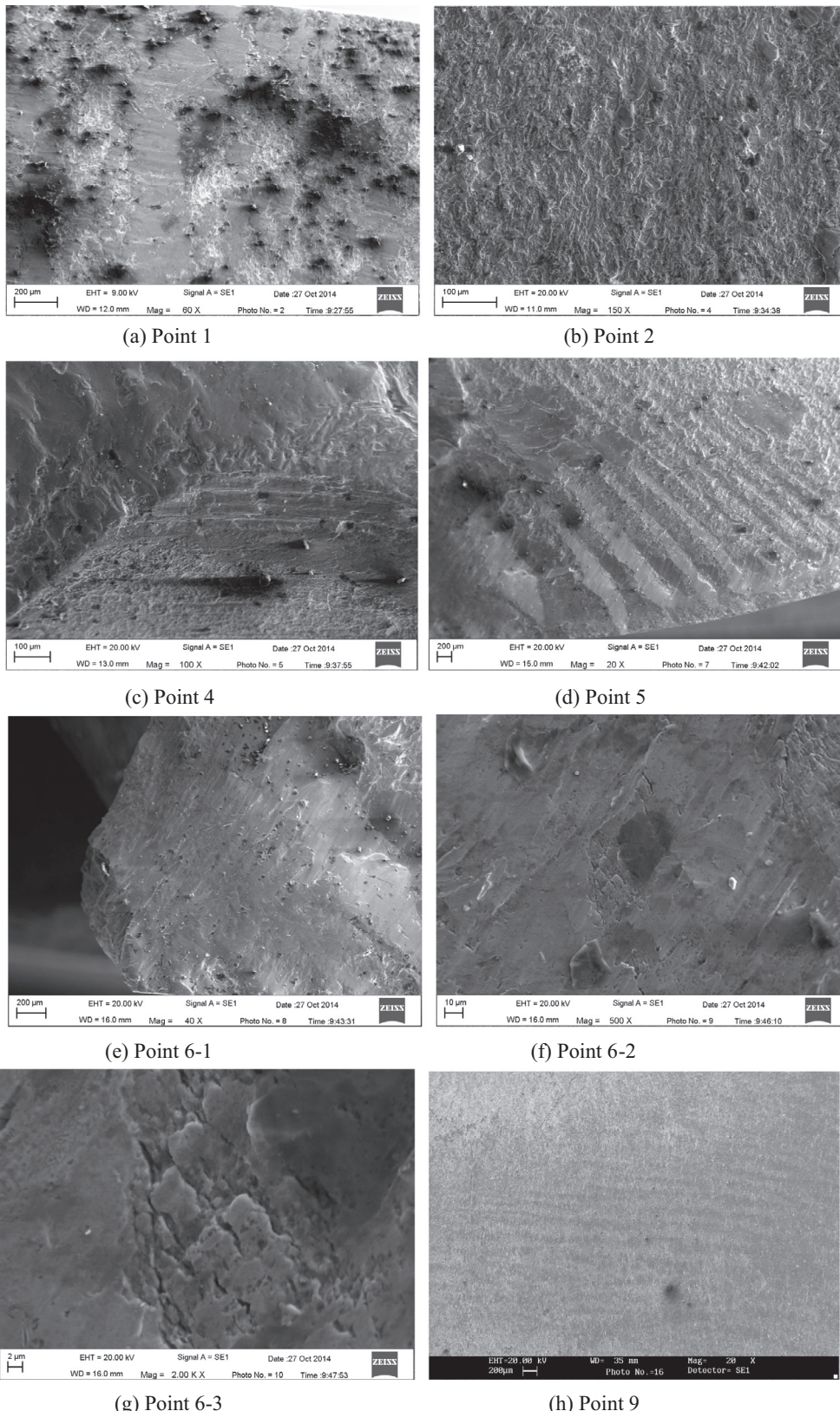


**Fig. 6.** Microstructure of the fracture surface.

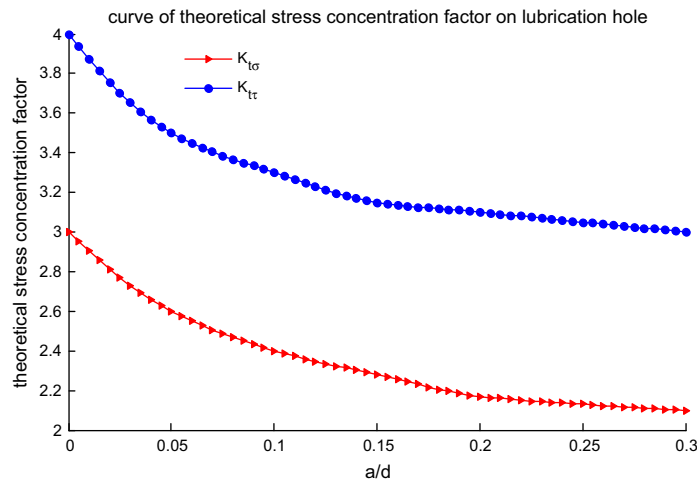


Fig. 7. Curve of theoretical stress concentration factor on lubrication hole.

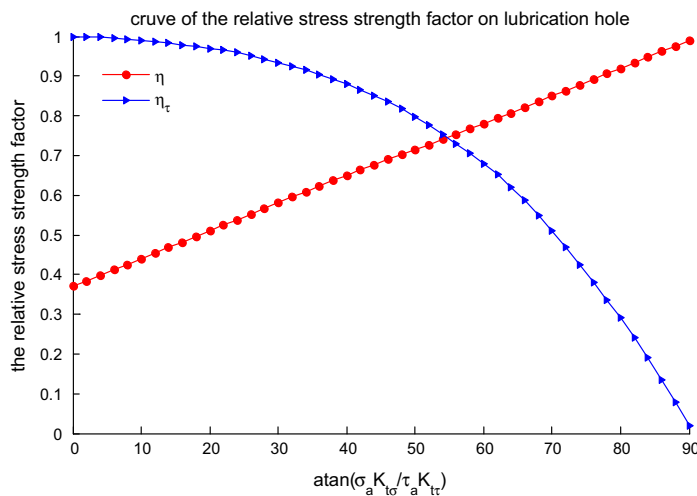


Fig. 8. Curve of the relative stress strength factor on lubrication hole.

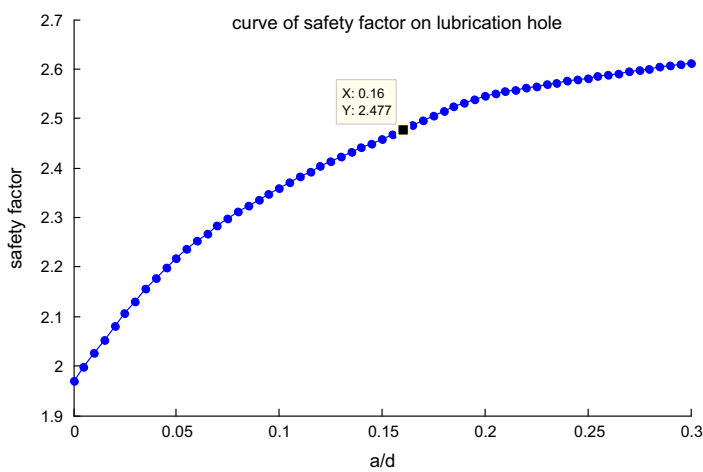


Fig. 9. Curve of safety factor on lubrication hole.

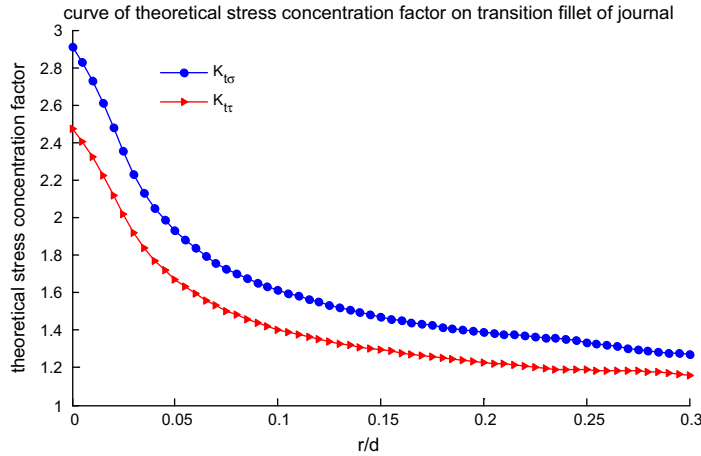


Fig. 10. Curve of theoretical stress concentration factor on transition fillet of journal.

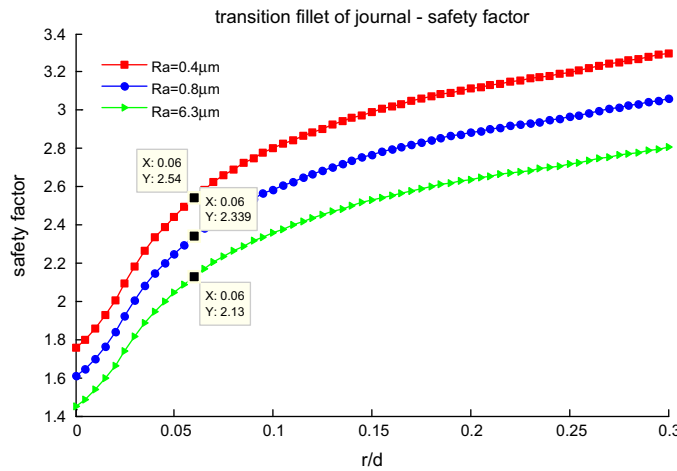


Fig. 11. Curve of safety factor on transition fillet of journal.

Table 3  
Safety factor and surface roughness.

r (mm)	R <sub>a</sub> (μm)	S <sub>ca</sub>
2	0.4	2.540
2	0.8	2.339
2	6.3	2.130

Here,  $\beta_1$  is surface quality factor,  $\beta$  and  $\beta_\tau$  are uneven stress distribution factors,  $S_\sigma$  and  $S_\tau$  are Safety factors under bending and torsion.

At first, the curve of theoretical stress concentration factor on the transition fillet of the journal through MATLAB simulation has been got which is shown in Fig. 10. The parameter  $r$  represents transition fillet radius of journal in Fig. 10.

Then the relationship between the safety factor, transition fillet of journal and surface roughness is found out and the curve is shown in Fig. 11 where  $R_a$  is surface roughness.

According to Table 3, the method to improve safety factor when the transition fillet has been large enough is found out which is reducing the surface roughness. The safety factor and surface roughness have been obtained where  $S_{ca} = 2.540$ ,  $R_a = 0.4 \mu\text{m}$  which is shown in part drawing, and the conclusion that fatigue strength on transition fillet of journal is in allowable range which is  $[S_{ca}] = 1.5-2.0$  can be drawn.

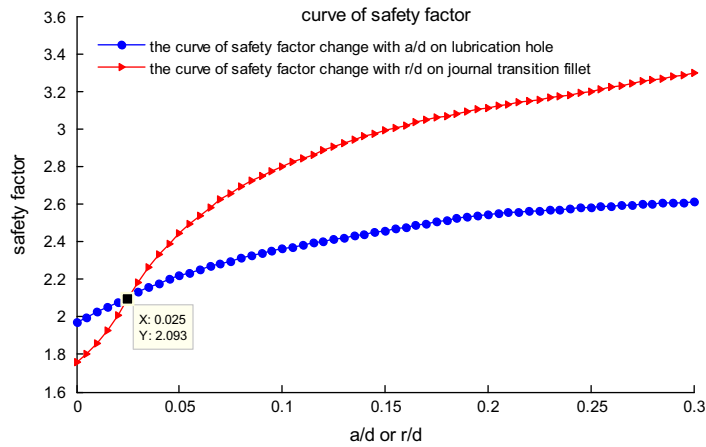


Fig. 12. Curve of safety factory.

#### 2.4.3. Fatigue strength analysis of the whole crankshaft

Based on the above safety factor calculation, the safety factors of the two dangerous sections have been compared where  $2.477 < 2.540$ . The result means that the dangerous section is on the surface of the lubrication hole on which the crack initially generated.

Then a comprehensive consideration of safety factor on surface of the lubrication hole and the transition fillet of journal has been taken into which is shown in Fig. 12.

The abscissa value 0.025 is a critical point from Fig. 12. When the abscissa value is greater than 0.025, the safety factor of transition fillet of journal is greater than the one on the lubrication hole and the dangerous section is on the surface of the lubrication hole. Through calculation we obtain that the critical radius is  $r = 1$  mm and the critical lubrication hole diameter is  $d = 1$  mm.

887799

# Materials safety: article exercise

You are working as a materials expert in your organization and your responsibility is to guarantee safe and efficient use of materials in your facility. One day, a failure in similar facility is brought to your attention, and you need to investigate the possible implications this failure has for your facility. Your job is to interpret and analyze the given failure report and to write a report, which will allow others in your organization to understand the key developments and causes leading to the failure and the necessary actions for prevention of such failures.

Read the given article and analyze the failure. Describe, how the deformation and failure mechanisms presented during the course are reflected in the case and establish the chain of actions leading to the failure. The report should work as an introductory material to your team; it should not be very long but it should enable other team members to understand the key features of the failure without reading the failure report itself.

In addition to establishing the primary cause of the failure, show why alternate failure mechanisms can be ruled out. Some failure mechanisms have not been discussed in the course yet. Conduct the analysis using your present knowledge on the subject.

If the author of the failure analysis has, in your view, neglected to address some aspects of the failure, you may indicate this in your report and suggest tests or actions that should have been done to clarify the issue.

Prepare your response by editing this word document and export it as PDF. The file name identifies you and the article. Do not change the file name (other than the extension to pdf). E-mail the pdf to "materials.safety@iikka.fi".

You may use the question list below to guide you in your analysis:

**A. Description of investigation methods applied**

- What means of investigation were used in the failure analysis?
- What computational methods were used?
- What material or results were obtained?

**B. The primary cause of the failure and description of the failure mechanism**

- What is the primary cause of the failure (also provide reasoning)?
- What's the chain of action that led to the failure?

**C. Ruling out alternate failure mechanisms**

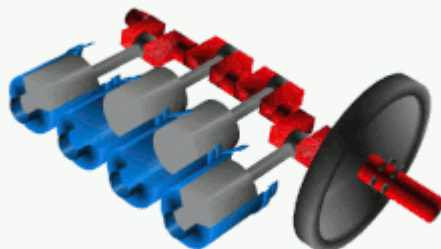
- Can plastic deformation be ruled out? If yes, explain how.
- Can creep be ruled out? If yes, explain how.
- Can brittle fracture be ruled out? If yes, explain how.
- Can fatigue be ruled out? If yes, explain how.
- Can environmentally assisted failure be ruled out? If yes, explain how.

**D. Recommendations to prevent similar failures in the future**

- How should the design, material, use, etc. be develop to avoid similar failures in the future? Provide several alternatives and indicate most promising.

Name: Nguyen Xuan Binh  
Student ID: 887799

### Materials Safety analysis report on the crankshaft fatigue failure



Crankshaft (red), pistons (gray), cylinders (blue) and flywheel (black)

#### Problem Overview:

The report investigated the reasons for the fracture of a crankshaft used in an air compressor. The focus was on understanding the cause of the fracture, especially considering the presence of beach marks with a semi-elliptical shape surrounding the fatigue crack initiation region. These marks were indicative of the expansion of the fatigue crack. The report provide insights into the fatigue behavior of 42CrMo steel under its cyclic operational conditions.

#### A. Description of investigation methods applied

- **What means of investigation were used in the failure analysis?**

From the report, the means of investigation for the failure analysis included:

1. Experimental analysis of the crankshaft: which consists of chemical composition detection, which reveals that the chemical composition of the main shaft was in accordance with the requirements of 42CrMo steel; and the crankshaft's mechanical properties.
2. Analysis of macroscopic and microstructural features: the microstructure of the crankshaft was analyzed around the lubrication hole and the transition fillet of the journal.
3. Theoretical calculations: derivation of safety factors for different sections of the crankshaft, such as the lubrication hole and the transition fillet of the journal.

- **What computational methods were used?**

The author lists a couple of computation methods as follows:

1. Scanning Electron Microscope (SEM) to confirm the fracture type and the initiation of crack source region, its propagation, and the cause of possible fracture.
2. MATLAB simulation: obtain the curve of theoretical stress concentration factor and the curve of the relative stress strength factor on lubrication hole

- **What material or results were obtained?**

**Main result:** The main results obtained are chemical composition detection, mechanical properties test, macroscopic analysis, microstructure of the fracture surface, analytical theoretical calculations of different properties of the broken crankshaft.

## B. The primary cause of the failure and description of the failure mechanism

- **What is the primary cause of the failure (also provide reasoning)?**

The primary cause of the failure was identified as the crack on the edge of the lubrication hole. The fracture surface was divided into three regions: fatigue crack initiation region, fatigue expansion region, and static fracture region. The catastrophic fracture, which indicates a high fatigue crack growth rate, seems to be a result of high bending. This high bending loading was attributed to the misalignment of the main journals and the small fillet of the lubrication hole.

- **What's the chain of action that led to the failure?**

The chronological order of the transmission towers' failure is as follows:

1. Initiation of micro cracks: micro cracks formed due to high bending stress concentration appeared on the fillet of the lubrication hole. However, the crankshaft continued to operate in a near-normal condition.
2. Fatigue crack extension: As the working time extended, the crankshaft began to exhibit noticeable fluctuations. The fatigue crack extended gradually, moving towards the static fracture region.
3. High bending stress concentration: This high bending loading was attributed to the misalignment of the main journals and the small fillet of the lubrication hole. This accelerates the fracture status of the crankshaft.
4. Complete fracture: eventually, the crankshaft fractured completely. At the moment of fracture, friction and collision occurred between the two fracture surfaces, leading to some degree of damage on the surfaces.

## C. Ruling out alternate failure mechanisms

- Can plastic deformation be ruled out? If yes, explain how.

No, plastic deformation cannot be ruled out. The report mentions high bending stress concentration at the fillet of the lubrication hole as a significant factor leading to the initiation of micro cracks. The stress concentrations can lead to plastic deformation

- Can creep be ruled out? If yes, explain how.

Creep can be ruled out due to the absence of prolonged high-stress levels. It's unlikely that the crankshaft experienced stresses conducive to creep.

- Can brittle fracture be ruled out? If yes, explain how.

Brittle fracture can be ruled out. The microscopic observation of the fracture surface using Scanning Electron Microscopy (SEM) does not reveal a brittle fracture surface.

- Can fatigue be ruled out? If yes, explain how.

No, it cannot be ruled out since it is the main reason stated in the report.

- Can environmentally assisted failure be ruled out? If yes, explain how.

Environmentally assisted failure can be ruled out. Environmentally assisted failures often exhibit specific features, such as corrosion pits, which were not observed on the crankshaft.

#### **D. Recommendations to prevent similar failures in the future**

- How should the design, material, use, etc. be developed to avoid similar failures in the future? Provide several alternatives and indicate the most promising.

To avoid similar failures in the future, several design, material, and usage recommendations can be inferred from the paper:

1. Material conditions: ensure that the chemical composition of the crankshaft material is in accordance with the requirements of the specific steel type (e.g., 42CrMo steel). Proper heat treatment and nitridation can enhance the mechanical properties of the material, making it more resistant to fatigue.
2. Regular inspections: implement regular inspections using SEM to detect early signs of fatigue or other damage. Early detection can prevent catastrophic failures.
3. Design modifications: address potential areas of high stress concentration, such as the fillet of the lubrication hole. Redesigning these areas to reduce stress concentration can significantly reduce the risk of fatigue crack initiation.

572266

## 1 Introduction

This report reviews a failure analysis that was conducted about a failed air compressor crankshaft. This crankshaft had failed by a fracture in two separate pieces from a surface in which a connecting rod is placed. The crankshaft was made of 42CrMo steel that was forged, heat treated, and nitrated. The failure analysis does not state how long the crankshaft had been used and only refers to the lifetime as "a period of time".

The overall air compressor mechanism operates as a common crankshaft-piston arrangement in which crankshaft rotates a connecting rod, that pushes a piston, and creates air pressure. Crankshaft transforms torque into linear movement and experienced compression, tension, and shear forces. According to author, the compressor is minor overload due to starting and stopping operating the compressor. The crankshaft has a detailed shape that introduces stress concentrators that are reviewed in detail in next chapter.

## 2 Investigation methods and failure mechanisms

The failed crankshaft was analysed by cutting the fractured section from the crankshaft. The following studies were conducted:

- Chemical composition by using a spectrometer (42CrMo alloy verified)
- Macroscopic fractography of fractured surfaces
- Microscopic inspection by using a scanning electron microscope (SEM)
- Mechanical material testing, such as tensile test, reduction of area, and hardness tests.

The author also calculated theoretical stress and safety factor values for the crankshaft. Here, MATLAB, was used to plot stress and safety factor curves.

By analysing the fractured surfaces visually on macroscopic level, the surface areas have obvious elements of failure by fatigue. Typical elements that can be identified from a fractured surface are:

- initial crack or nucleation (a crack or some abnormality within the surface),
- progression marks (a geometric pattern, such as lines), and
- fracture region (a separate surface from progression area with its own surface marks).

Pictures from the fracture surface suggests that the fatigue initiated from a region next to a lubrication hole that seems to have a rough surface and a chamfered edge. The overall point of fracture seems to be located in a vulnerable spot between a rounded edge of a connecting rod neck and a lubrication hole.

The microscopic analysis also suggests failure by fatigue as the three typical areas of initiation, progression, and final fracture. Pictures using SEM shows very fine progression marks around the fracture surface that cannot be otherwise seen.

Mechanical test such as tensile test, measure of reduction area, and hardness test were conducted. The material was verified as 42CrMo by spectrometer and the alloying elements are within the specification. Mechanical test show that the material properties are within tolerances. The steel should not be to brittle i.e., hard, that would make the part vulnerable for other types of failures such as brittle fracture. The author does not mention how the test were conducted and what specimen were used.

### 3 Failure analysis

By combining all evidence from the author's investigation, the most likely primary failure mechanism has been a fatigue. The chain reaction in this case is simple as there is no evidence of other failure mechanisms present.

During operation, the air compressor is started, operated, and stopped. During normal operation, the load during one compression cycle is smaller but number of cycles is large. This is opposite with starting and stopping the compressor in which load is higher with starting and stopping cycles but number of them is low. This simultaneous cyclic loading can be seen as minor progression marks (seen using SEM) and larger progression marks next to initiation area (seen on macroscopic level).

The theoretical loading and safety factors were calculated. The overall safety factor within the fracture region was over 2 regarding all the stress concentration elements. The author calculated that the surface roughness decreases fatigue strength safety factor. The author calculated that 0.4 µm average surface roughness the safety factor is 2.54 on top of connecting rod neck. However, the lubrication hole has a marked average surface roughness of 12.5 µm that would decrease the safety factor. The author calculated that average surface roughness of 6.3 µm would result as a safety factor of 2.13.

There are still other failure mechanisms that should be addressed and possibly ruled out as a possibility. Some of them are listed here:

- Plastic deformation can be ruled out as primary failure mechanism. The macroscopic and microscopic analysis does not suggest that there has been a ductile fracture. The crank-shaft has not plastically deformed. There are microscopic marks of plastic deformation in the final fracture surface.
- Creep can be ruled out. There are no signs of cracks on microscopic level that would suggest failure by creep. The fracture on macroscopic level does not suggest failure by creep. The author does not mention of operational temperatures.
- Brittle fracture can be ruled out as primary failure mechanism. Mechanical testing suggests that the material is not susceptible for brittle fracture mechanisms. The fracture surface does not show marking of brittle fracture.
- Fatigue has been proposed as primary failure mechanism.
- Environmentally assisted failures can be ruled out as there is no sign of corrosion and elevated temperatures were not mentioned in the failure analysis.

For future recommendations, part design should be re-evaluated. There are significant mechanical vulnerabilities in the fracture region that act as stress concentrators. The failure analysis does not mention if the combined effect of these elements has been considered. Surface roughness of lubrication hole is not discussed in the failure analysis. The primary action should be the re-evaluation of safety factor overall.

100501616

# Materials safety: article exercise

The report assesses the failure of a crankshaft made of 42CrMo steel with forging. The crankshaft fractured after a period of use. The analysis approaches by three methods: experimental analysis, macroscopic and microscopic analysis, and theoretical calculations.

The experimental analysis studies the chemical composition of the crankshaft and the mechanical properties. The chemical composition and the mechanical properties results agree with the standard requirements. The macroscopic analysis investigates the fracture surface and divides it into three regions: fatigue crack initiation region, fatigue expansion region, and static fracture region. The beach marks with semi-elliptical shape near the lubrication hole indicate a fatigue failure. It shows that the fracture was caused by fatigue crack due to the misalignment of the main journals and the small fillet of the lubrication hole. This misalignment resulted in high bending stress concentration, which led to fatigue crack initiation on the edge of the lubrication hole. In the beginning of the fatigue expansion region, there are also beach marks created from the compressor operation. The static fracture region is where the final failure occurs. The microscopic analysis used SEM to observe the fracture surface at critical points. This analysis tells about the fracture type and initiation points and also confirms the cracks started from the edge of the lubrication hole. Theoretical calculations were done for the fatigue strength on the lubrication hole, the fillet of the journal, and the whole crankshaft.

The chain of action led to failure can be described as follows: The lubrication hole and the journal were misaligned, causing high bending stress concentration during operation. After some numbers of cycles, microcracks initiated on the fillet of the lubrication hole. As the crankshaft operated, the cracks grew to the start of the static fracture region and then the crankshaft fractured completely. The two fractured surfaces collided and causes damage on the surface due to friction.

The main cause of failure is fatigue on the fillet of the lubrication hole. Other mechanisms such as plastic deformation, creep, brittle fracture and environmentally assisted failure can be ruled out in this case. The



analysis clearly showed beach marks and fatigue crack initiation point which strongly indicate fatigue failure.

To prevent similar failure, we can improve the design or material used, and control the quality of the part before operation. The report points out that the main reason for failure is due to the misalignment between the hole and the journal. Thus, it is most practical to carefully do the quality checks and alignment check, making sure that every component works properly as their design.



## **1. Introduction**

Life time of real components is defined by a broad range of manufacturing, design and service factors. Compressors are one of the main components of oil and gas industries. The major function of a compressor is to compress air which is used in combustion process. Compressors use arrays of fan-like air foils to progressively compress the working fluid. Compressor blades are variously made by forging, extrusion or machining. These blades play important role and are designed to operate at high temperatures and aggressive environments and are subjected to high rotational velocity which results in high centrifugal forces on the blades. Cyclic loading causes the blades to metallurgically and mechanically degrade during service which limit their useful life service. In sea water environment, corrosion pits can appear on the blades. These corrosion pits can have detrimental influence on the fatigue strength of the material and raise the stress level locally. It is reported in the most of corrosion fatigue failures of components, cracks initiate from corrosion pits [1,2]. Becker et al. [3] reported the effect of pitting corrosion on fatigue and fracture behavior of 13% Cr stainless steel and studied the interactive effects of corrosion pit nucleation and growth. Philips and Newman [4] established the importance of short crack analysis and used Paris law for crack growth in Al 2024-T<sub>3</sub> alloy. During stress fluctuations the crack propagates and reaches the critical size, leading to sudden rupture. Failure due to initiation and propagation of fatigue cracks originating from service defects is typical of compressor blades and has been investigated by researchers [5–7]. The reliability and performance of a gas turbine compressor is strongly dependent on the environment in which it operates and the materials that are used. In the past, the blades were made of coated AISI403 stainless steel. As far as the coating is worn away on the pressure side of the blades, in 1980s they were substituted with GTD-450 alloy. This is an age-hardenable, martensitic stainless steel. It has the strength characteristics of a martensitic stainless steel combined with corrosion resistance which is comparable to an 18Cr-8Ni stainless [8,9]. The objective of the presented study is to

Chemical analysis of the fractured blade.

Chemical analysis of the fractured blade												
Elements	C	Si	Mn	P	S	Cr	Ni	Mo	Cu	Al	Nb	Fe
Result	0.029	0.22	0.58	0.003	0.005	15.00	6.25	0.75	1.72	0.01	0.32	Rem.
GTD 450 alloy	*	*	*	*	*	14.00	5.00	0.5	1.25	*	0.04	Rem.
Min.	*	*	*	*	*	14.00	5.00	0.5	1.25	*	0.04	Rem.
Max.	0.05	1.00	1.00	0.03	0.03	16.00	7.00	1.00	1.75	*	*	Rem.

investigate the reason for sudden and early failure of a gas compressor blade working for about 34,000 h at sea water environment. Note that according to the blade manufacturer their working life is about 48,000 h to 100,000 h depending on environment and blade surface modification.

## 2. Materials and methods

### 2.1. Chemical analysis

Chemical analysis of the fractured blade was done by emission spectrometry. The results are shown in [Table 1](#). According to this analysis, it was found that the blade material is consistent with GTD-450 alloy analysis which is a common alloy for fabricating gas compressor blades.

### 2.2. Mechanical tests

According to the supplier documents, the blades have been age hardened at H1000 condition. In this condition age hardening is performed at 1000 °F or 540 °C for about 4 h. In order to be confident about the mechanical characteristics of the blades at H1000 condition and compare it with the standard values, hardness test and tensile test were performed on the crack free blades.

#### 2.2.1. Hardness test

Brinell hardness measurements were carried out on the polished cross section of the blades using 30 kgf load. The average hardness of the three different locations was reported.

#### 2.2.2. Tensile test

Tensile test was performed at room temperature by a Gotech machine based on ASTM E8 standard [\[10\]](#). The average value for ultimate strength, yield stress, percent elongation and percent reduction in area is taken after testing two specimens.

### 2.3. Microscopical investigation

The metallographic specimens obtained were rubbed with 120–2000 mesh sand paper, as a result, their surface were cleaned and the cross sectional surfaces were polished by 3 µm diamond paste and solvent. For microstructural examination the specimens were etched with a solution of 1.5 g CuCl<sub>2</sub>, 33 ml hydrochloric acid, 33 ml ethanol and 33 ml distilled water. A scanning electron microscope (SEM) was used to evaluate the microstructure of selected samples. X-ray analyses (EDX) of selected areas were also obtained.

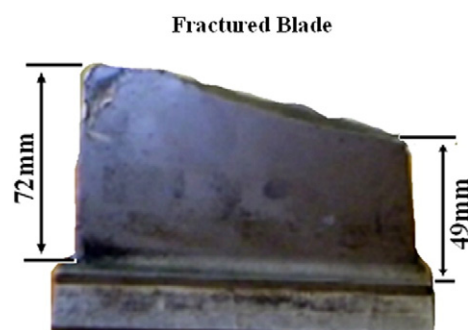


**Fig. 1.** The fractured blade and the failure location on it.

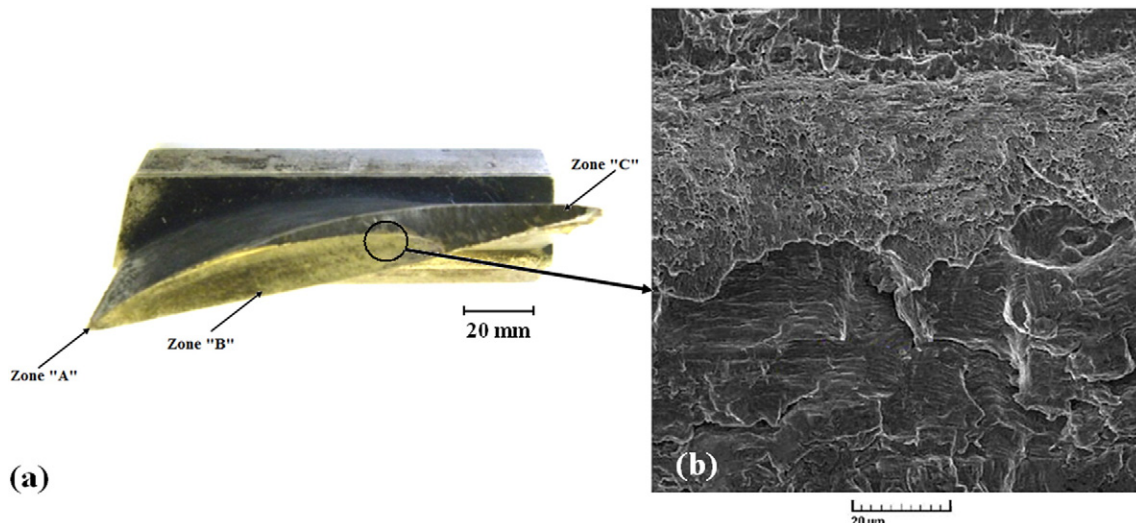


**Fig. 2.** (a) Macroscopical investigation on the fractured blade with three different zones and (b) SEM micrograph of transition from zone (B) to zone (C) on the fractured blade.

### 3. Results and discussion

#### 3.1. Visual examination of failed blade

The fractured blade was first subjected to visual examination.

The blade failure location is presented in Fig. 1. As it is seen, the blade fracture zone is 72 mm above the blade root on the left side and 49 mm above the blade root on the right side. The macroscopical investigation on the fractured blade in Fig. 2a reveals the existence of three different zones. Crack origination site at zone (A), beach marks associated with fatigue crack propagation at zone (B) and brittle fracture at zone (C). Fig. 2b demonstrates the SEM micrograph of transition from zone (B) to zone (C). It means that fatigue cracks have propagated in a way that they have reached their critical size and brittle fracture has occurred, finally.

#### 3.2. Mechanical test results

**Table 2** presents the hardness results from different parts of the blade such as convex area, core of the blade and concave area. The average hardness value is consistent with the standard limits. The least allowable hardness for the specified material at H1000 condition is 331HB [11].

**Table 3**, shows the tensile test results for the blade. It is obvious that the percent elongation, percent reduction in area and yield stress are in good consistence with ASTM A705/A705M [10] specification for this alloy at H1000 condition. However, ultimate tensile strength is a little lower than the standard limits.

**Table 2**

Hardness results from different parts of the blade.

Regions	Hardness (HB)			
	Point 1	Point 2	Point 3	Average
Convex area	348	350	345	348
Core of blade	366	360	362	363
Concave area	331	341	335	336

**Table 3**

Tensile test results for the blade.

Sample	D (mm)	Cross section (mm <sup>2</sup> )	Yield strength (MPa)	Ultimate strength (MPa)	Elongation %	Reduction in area (%)
GTD450 alloy	6.32	31.4	1034	1071	20	73
ASTM A705	-	-	Min.1030	Min.1100	Min.12	Min.45

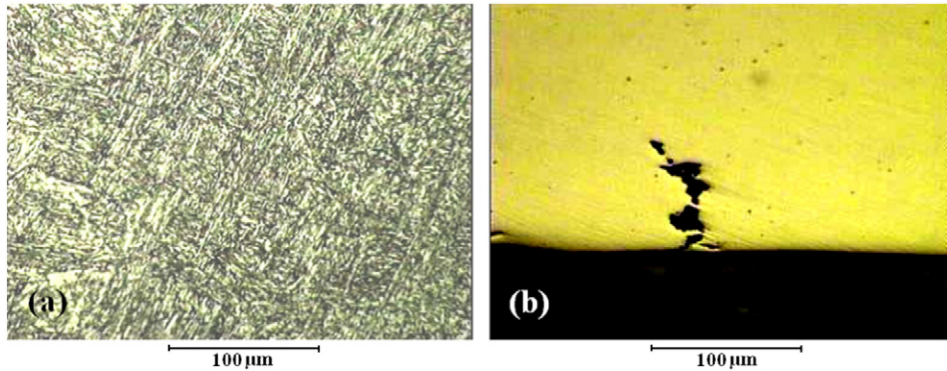


**Fig. 3.** Optical micrograph from the surface of the blade. (a) The etched surface of the blade and (b) the corrosion pits on the blade surface.

### 3.3. Microscopical analyses

In order to verify possible corrosion aspect, a cross section near the fracture initiation area was prepared for metallographic examination. Fig. 3a, b presents the optical micrographs from the surface of the blade. According to Fig. 3a one can see that the etched surface of the blade consists of tempered martensite in a ferritic matrix which is a common microstructure for martensitic stainless steels. Fig. 3b demonstrates the corrosion pits on the blade surface which have nucleated due to corrosive environment.

In order to better follow the nucleation and initiation of cracks from these corrosion pits, scanning electron microscope (SEM) was used. Fig. 4a shows the cross section of the blade near the crack initiation site. In this figure the depth of a corrosion pit is seen which has been surrounded by several micro cracks. In this case the depth of the corrosion pit can be assumed as the initial crack length which is about 20  $\mu\text{m}$  [12]. Fig. 4b presents the fracture surface of the blade after 34,000 h work with microscopic pits near the surface as shown by an arrow.

According to [13] the initiation and growth of corrosion pit, crack initiation from a corrosion pit and the fatigue crack propagation are the key characteristics to judge corrosion fatigue failure. Corrosion pits in Fig. 5 produce a characteristic grain boundary attack. It can cause an intergranular separation of crystals. This morphology of fatigue failure is typical for weakening the grain boundaries by corrosion. Corrosion pits are electrochemically active and once formed, act as stress concentration site and can facilitate crack initiation under cyclic loading.

EDX analysis which was performed on precipitates in the corrosion pits and also on the cracks at fracture surface of the blade shows the presence of chloride ion as a corrosive agent. Fig. 6a, b demonstrates the EDS analysis of the corrosion products in the pits and on the fracture surface of the blade, respectively. The acidity of the electrolyte inside the pits increases by increasing the chloride ion which causes further acceleration of corrosion process.

Fig. 7a presents the micrograph on the fracture surface of the blade. The river lines are obviously visible on the surface. These river lines are along with the direction of fatigue crack propagation. SEM micrograph of the fracture surface in Fig. 7b shows typical fatigue striation spacing taken at a distance of 82 mm from the crack origin site. Striation profiles are characteristic of the amount of deformation the material can absorb prior to fracture. According to [14], these striations are brittle striations which have appeared

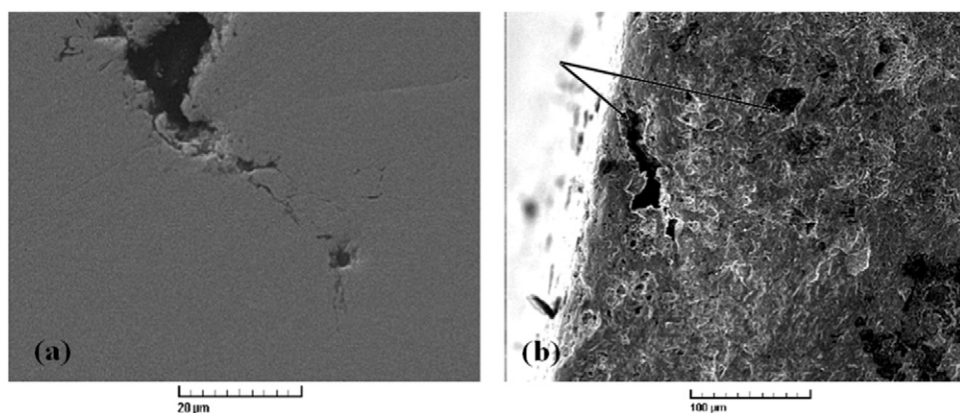


**Fig. 4.** (a) Cross section of the blade near the crack initiation site with a corrosion pit surrounded by several micro cracks. (b) The fracture surface of the blade after 34,000 h work with microscopic pits near the surface.

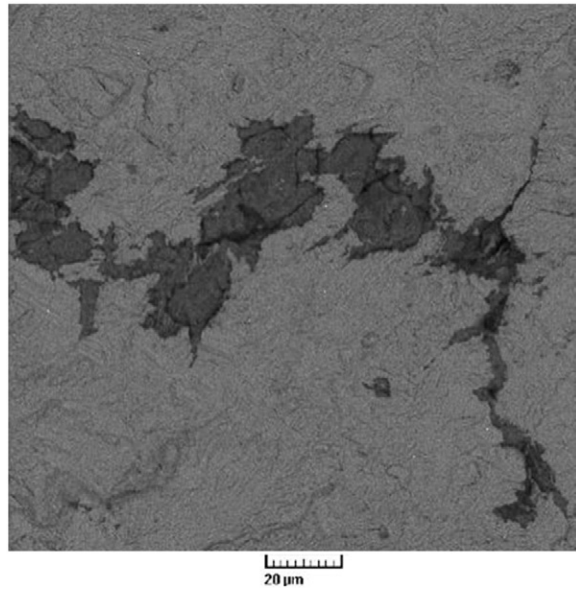


**Fig. 5.** SEM micrograph of intergranular fracture of the blade.

as concentric circles departing from the initiation site and are always associated with corrosion assisted fatigue. A characteristic feature of brittle striation is the uniform, flat and woody year-ring propagation. The concentric circles in Fig. 7b show the overload marks [15] just to open crack tip and mark the growth. A non-uniform pressure distribution of fluid or the loss of the blade material which may produce an unbalance on the rotor can lead to overload on the blade.

The repetition of tension–compression cycles in compressor blade leads to generation of a continuous path along which damage accumulates and eventually becomes a micro crack (Fig. 8a) and advances in a zigzag mode (Fig. 8b) in a direction perpendicular to external load. Note that fatigue striation spacing at Fig. 8a is taken at a distance of 40 mm from the crack origin site. It can be concluded according to [1,16] that crack initiation process can be accelerated by torsional vibrations. It means that under vibrations the stress level in the crack initiation zone is much higher than the stress level results from blade rotation. So vibrations (torsional or transverse) are more dangerous than oscillated rotation.

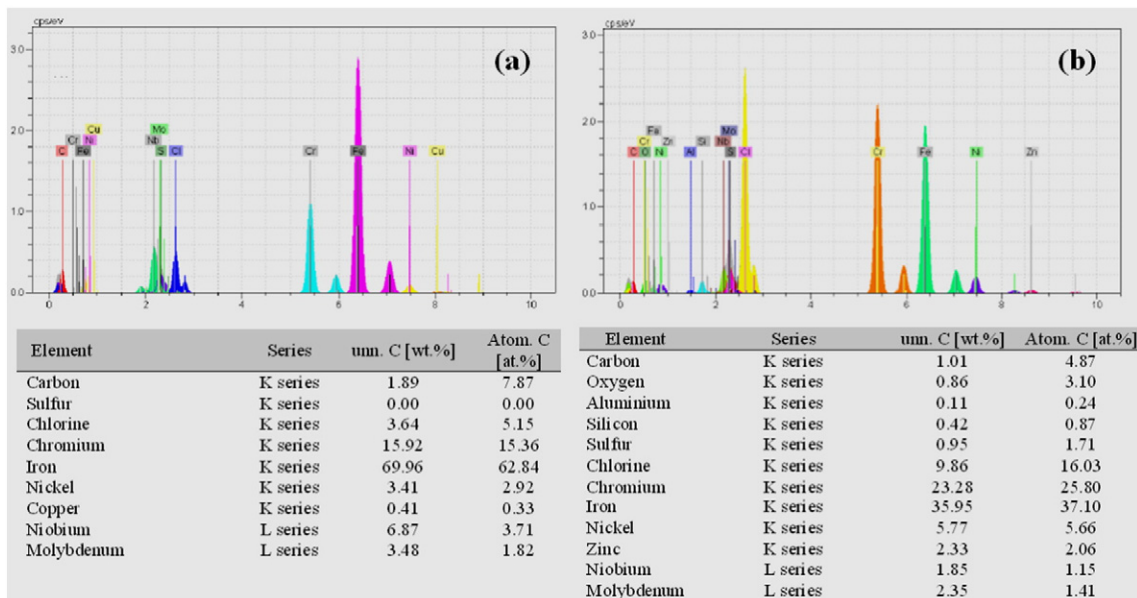


**Fig. 6.** EDS analysis of the corrosion products (a) in the pits and (b) on the fracture surface of the blade.

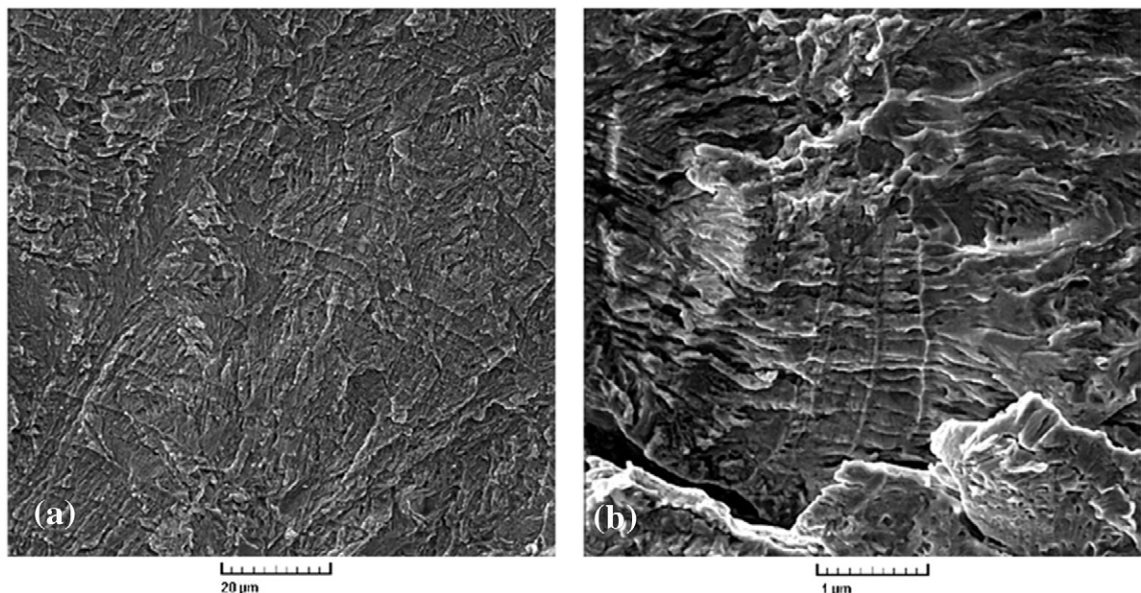


**Fig. 7.** (a) SEM micrograph on the fracture surface of the blade with river lines. (b) Typical fatigue striation spacing taken at a distance of 82 mm from the crack origin site.



100509058

## 1 Introduction:

Air compressors are essential components in the oil and gas industries. They function by compressing air using rapidly rotating blades. These blades are typically made through processes like forging, extrusion, or machining. One common problem that affects these blades is wear and tear caused by repeated use. The environment in which the blades operate can have a significant impact on how long they last. Previous studies have revealed that the operating conditions can lead to corrosion on the blades, which can increase localized stress and reduce the overall lifespan of the blades. In this specific case, researchers investigated why a gas compressor blade, expected to operate for 48,000 to 100,000 hours as per the manufacturer's guidelines, failed after only 34,000 hours of use.

## 2 Methods:

The researchers used various methods to determine the primary cause of the blade's failure. They conducted a chemical analysis of the fractured blade using emission spectrometry. Additionally, they performed hardness and tensile tests on the broken blade to validate the manufacturer's claim that the blades had been age-hardened at H1000 condition. For the hardness test, a Brinell hardness test was conducted on the polished surface of the blade using a 30 kgf load, and the tensile test was carried out at room temperature.

Furthermore, the researchers prepared metallographic specimens by employing both mechanical and chemical preparation techniques on the fractured blade. These prepared samples were then examined using scanning electron microscopy (SEM). X-ray analyses of selected area were also obtained.

## 3 Results and discussion:

Upon a visual examination, the researchers identified three distinct areas on the fracture surface. These areas included the zone where the crack initially began, the region where the crack continued to grow, and the area where the fracture displayed a brittle appearance. SEM images further supported this observation, as they revealed a transition from the propagation zone to the brittle fracture zone. This indicated that the fatigue crack had extended to a critical length, ultimately leading to a brittle fracture.

The chemical analysis indicated that the blade was constructed from GTD-450 alloy, a widely used material in blade manufacturing.

The hardness test was conducted on various sections of the blade, and the outcomes were consistent with the specified hardening condition. Specifically, the minimum hardness required for H1000 hardening condition should exceed 331HB, and all test results exceeded this threshold. Furthermore, the results from the tensile test aligned with the stated hardening condition. Parameters such as percent elongation, percent reduction in area, and yield stress were well within the specifications for the GTD-450 alloy at H1000 condition. However, it's worth noting that the ultimate tensile strength fell short of the standard limit.

Under optical microscopy, the metallographic specimens displayed corrosion pits on the surface of the blade. Subsequent SEM images of these specimens revealed the presence of multiple micro cracks surrounding these corrosion pits. The researchers determined that the depth of the corrosion pit, which measured at 20 $\mu\text{m}$ , represented the initial crack length. Further SEM images of the fractured surface indicated that the corrosion pits had caused a distinctive grain boundary attack. As a result, they concluded that these corrosion pits were electrochemically active, serving as stress concentration points and contributing to both the initiation and propagation of cracks during cyclic loading.

The EDX analysis conducted on the corrosion pits and cracks present on the fracture surface detected the presence of chloride ions as the corrosive agent. Interestingly, the quantity of chloride ions inside the pits was greater than that found within the cracks on the fracture surface. This disparity led to a more acidic environment within the pits, accelerating the corrosion process.

SEM imaging was employed to examine the fractured surface, and it unveiled that typical fatigue striations were spaced at intervals of 82 mm from the crack's point of origin. The shape of these striations indicated that they were brittle in nature.

In conclusion, the researchers determined that the cyclic loading process resulted in the formation of microcracks. These microcracks advanced in a zigzag pattern, perpendicular to the external load. Additionally, they noted that, apart from the corrosive pits, torsional vibrations played a role in speeding up the propagation of these cracks.